



Assessment of the influence of an Australian native eucalypt, *Corymbia maculata*, on soil desiccation in a temperate climate

Xi Sun¹ · Jie Li¹ · Donald Cameron¹ · Annan Zhou¹ · Peter Bayetto² · Gregory Moore³

Received: 21 August 2022 / Accepted: 3 September 2023 / Published online: 26 September 2023
© The Author(s) 2023

Abstract

Expansive soils undergo significant moisture change under prevailing climate conditions, resulting in shrinkage and swelling in dry and wet months. Such seasonal movements of expansive soils can greatly affect the serviceability and performance of lightweight structures founded on shallow footing systems. The extent of movement may be exacerbated if trees are present since large amounts of water can be absorbed by the root system of trees, leading to localized settlement due to soil shrinkage. This study established a well-instrumented site that included a row of Australian native eucalypts located in an eastern suburb of Melbourne, Australia. A tree from this row was chosen for the monitoring of soil movements, soil moisture and suction over a period of 44 months. A sap flow instrument was used to monitor the transpiration and water uptake by the tree. The results showed that noticeable shrinkage settlement occurred at a radial distance of 7.8 m from the trunk of the tree, attributable in part to the increased water demand of the tree. This study promotes a better understanding of the process of expansive soil–tree root interaction. The field data presented can assist geotechnical engineers and practitioners with footing design in the presence of trees.

Keywords Eucalypt · Expansive soil · Ground movement · Sap flow · Soil moisture · Soil suction

1 Introduction

Trees enhance the liveability of cities and make urban environments more sustainable for residents. Trees also provide an aesthetic touch to local areas and improve the design of a streetscape. Trees planted on the street verge can increase the median property value of a house by approximately 1.9% in Western Australia and more in Queensland [31, 32]. On the other hand, trees can extract moisture from soils, leading to soil desiccation and causing localized differential movements which can cause stresses that damage structures above ground as well as underground utilities [8]. Trees extend their roots as far as possible to survive when water is not readily available. The size of the tree root system is mainly dependent on the availability of soil moisture. Sufficient water supply may lead to a smaller extent of tree roots, while roots can proliferate to a greater depth and extend significantly away from the tree trunk when soil water is limited [13]. Tree roots exert suction forces on soils in their vicinity and may cause deep drying. Ng et al. [30] studied the influence of plant morphology on soil–tree root hydraulic interactions

✉ Jie Li
jie.li@rmit.edu.au

Xi Sun
xi.sun@rmit.edu.au

Donald Cameron
Donald.Cameron@unisa.edu.au

Annan Zhou
annan.zhou@rmit.edu.au

Peter Bayetto
bayetto@internode.on.net

Gregory Moore
gmmoore@unimelb.edu.au

¹ School of Engineering, RMIT University, Melbourne, VIC 3001, Australia

² FMG Engineering, Adelaide, SA 5034, Australia

³ School of Ecosystem and Forest Sciences, Burnley College, University of Melbourne, Melbourne, VIC 3021, Australia

for 26 individual *Schefflera heptaphylla* and found the ability of tree water uptake stayed at the maximum level before wilting point soil suction (i.e. soil suction above which tree roots cannot continue to extract water from the soil) is reached and was positively correlated to the ratio of leaf area to root length. Through the study of soil suction close to trees in Adelaide, Australia, Cameron [7] concluded that the effect of root-induced soil drying can extend to a depth of approximately 4 m for an individual tree, while trees in groups can extract water from 6 m deep due to competition with neighbouring trees [9]. Blight [4] showed that the lateral influence of poplar trees on soil moisture conditions in South Africa extended to 7.5 m.

Garg et al. [16] conducted a study in Hong Kong, a subtropical climate region with hot and humid summer months, to investigate soil suction distribution in recom-pacted slopes planted with Bermuda grasses and Ivy trees. They concluded that the highest tree-induced soil suction was 700 kPa, which is approximately 72% higher than the suction caused by grasses during dry months. In another study, Garg et al. [17] compared the soil suction caused by evapotranspiration and transpiration of *Schefflera heptaphylla* and found that the tree can significantly affect soil suction distribution, particularly within the tree root-affected zones. The evapotranspiration-induced soil suction could be as much as 47% greater than tree-induced transpiration. Gadi et al. [15] investigated the correlation between soil suction and stomatal conductance of grass species, *Axonopus compressus* and *Cynadon dactylon*. They concluded that stomatal conductance increases with a rise in soil suction up to 6 kPa due primarily to the increase in oxygen levels within the pores of the soil–root composite. A significant reduction of more than 90% in stomatal conductance was observed for suction ranging between 6 and 1340 kPa. At the wilting point soil suction of 2431 kPa, stomatal conductance is 0 mmol/m/s. Zhou et al. [39] assessed soil suction distribution near *Elaeocarpus apiculatus* Masters and *Pink Shower* trees grown in an urban site, taking into account the impact of termite infestation and radiation intercept by the canopy of trees. They found that, before termite infestation, soil suction at shallow depths was the highest in close proximity to the tree stem, which decreased with distances up to 3 m away from the tree due to the effect of canopy shading. However, after termite infestation, soil suction decreased substantially near the tree stem and increased farther away as a result of the reduced canopy area and stomatal conductance caused by the infestation of the trees.

In Australia, studies have been undertaken into expansive soil behaviour from the late 1950s and the outcome is the development of a standard for the design of residential slabs and footings. The Australian Standard AS2870—Residential Slabs and Footings was initially released in

1986 to counter the disparate practices existing before that time throughout Australia and even across suburbs in cities. The Standard was revised in 1988, 1996 and 2011 [23]. Guidance for designing footings in close proximity to an individual tree or a group of trees was not provided in all versions of the Standard, until the 2011 version. Instead, proximity rules were introduced relating safe distances between buildings and trees based on tree height; it was recommended trees should be kept as far as possible from residential buildings so that the influence of trees on the movement of footings could be minimized. It was suggested that for a single tree, the influence of tree root drying might be ignored if the distance between the tree and the footing was equal to the mature tree height (HT). This distance was increased to $1.5 HT$ and $2 HT$ for a group of trees and a row of trees (4 or more), respectively. Trees found within these distances were considered to be outside the scope of the earlier versions of the Standard. More information on what is provided in AS2870 [3] is discussed later.

The latest edition of the Australian Standard [3] classifies sites into one of five categories based on the characteristic ground surface movement y_s (Table 1). The design surface movement is dependent on the soil profile and the influence of local climate on soil moisture level and is calculated by summing the movements for all layers from the ground surface to the depth of design suction change (H_s) (Eq. 1).

$$y_s = \frac{1}{100} \sum_{n=1}^N (I_{pt} \overline{\Delta u} h)_n \quad (1)$$

where I_{pt} is the instability index and is obtained by multiplying the correction factor α (ranging from 1 to 2) by a shrinkage index I_{ps} ; $\overline{\Delta u}$ is the averaged design soil suction change for the soil layer; N is the number of layers within the depth of H_s ; and h is the thickness of the soil layer. Sub-layers of soil horizons are commonly applied.

Design soil suction change for “no trees” is shown in Fig. 1. Δu_s is the maximum surface design suction change, and a value of 1.2 pF is given in AS2870 [3], representing

Table 1 Site classification based on y_s near the *C. maculata* tree

Characteristic ground surface movement (y_s) mm	Reactivity (Class)
0–20	Slight (S)
20–40	Moderate (M)
40–60	High (H1)
60–75	Very high (H2)
Greater than 75	Extreme (E)

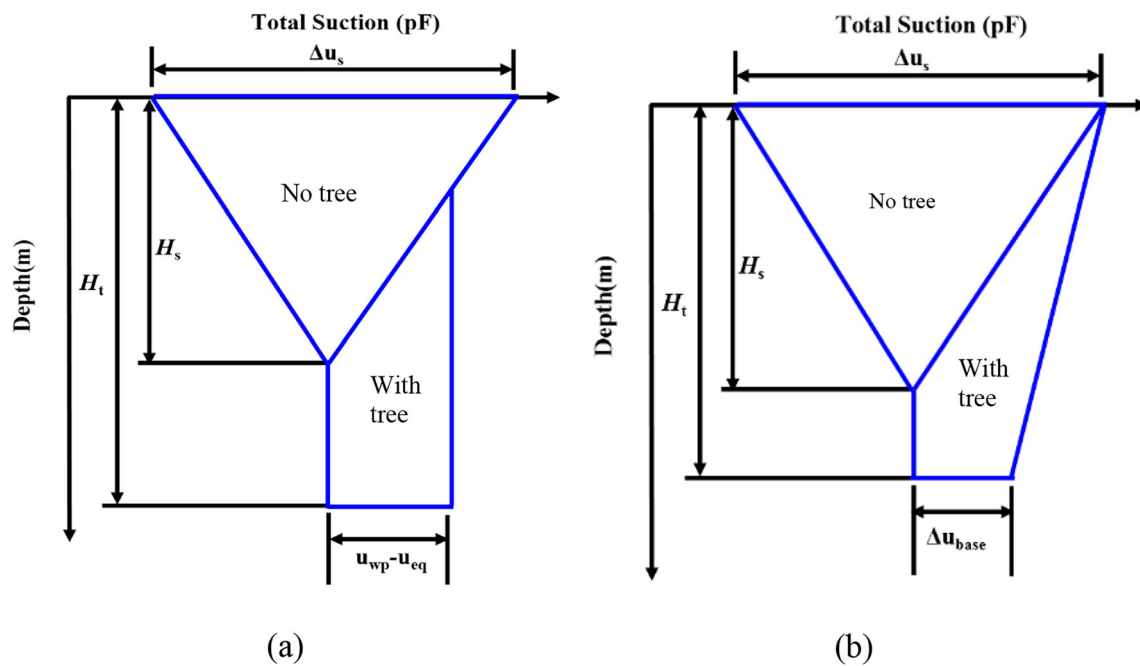


Fig. 1 Design suction change profile for the effect of trees [3]: **a** theoretical suction change distribution and **b** equivalent suction change distribution

a change in total suction (e.g. 3.3–4.5 pF or 195 kPa–3.09 MPa). The design suction change was assumed to decrease linearly with depth and become zero at H_s , below which no suction change occurs in response to site environmental changes from building houses on green sites. Long-term moisture re-distribution follows the development of a building site. The depth of H_s is climate dependent.

In 2011, the Australian Standard [3] introduced an additional design soil suction change profile (Fig. 1) to accommodate tree drying. An informative appendix gave additional design suction changes and a greater depth of suction change to cater for the effect of tree root drying for footing design. As shown in Fig. 1, the drying depth extended from H_s to H_t due to the effect of trees. Figure 1a illustrates the wilting point suction concept wherein soil at depths below the normal design suction change envelope cannot have suctions greater than the wilting point suction for those trees [9]. The tree-induced suction change could be estimated by subtracting the deep equilibrium soil suction u_{eq} (a long-term soil suction that would not change as a result of climatic variations) from the wilting point soil suction u_{wp} . The area of additional drying due to the tree effect in Fig. 1a was converted to a more convenient equivalent suction change distribution shown in Fig. 1b by the technical committee for the Standard. The shape of the extra design suction change (Fig. 1b) is an approximation to what should be expected on site. For design purposes, the Australian Standard provides conservative values of the

maximum extra suction change Δu_{base} for different depths of H_s and H_t for both the single tree and groups of trees and assumes that Δu_{base} and H_t are dependent on H_s and the number of trees. The actual Δu_{base} may exceed the values introduced in the Standard if trees dry the soil to the wilting point value in wetter climates, leading to an underestimation of soil movement caused by trees [9].

The additional ground movement y_t due to tree drying of soils is calculated using Eq. 2, assuming that the soil profile is fully cracked, and thus α is taken as 1 throughout the calculation. The value of y_t assumes very close trees and a reduction is allowed based on proximity, according to Eq. 2:

$$y_t = \left[1 - \left(\frac{\frac{D_t}{HT} - 0.5}{\frac{D_i}{HT} - 0.5} \right) \right] y_{t_{max}} \quad (2)$$

where D_t is the distance between the tree and the building; D_i is the influence distance of the tree; HT is the tree height; and $y_{t_{max}}$ is the maximum potential soil movement due to the effect of the tree and is calculated according to Eq. 1. The guideline for estimating tree-induced extra soil movement is simplistic and based on limited experimental data from too few sites with total suction profile data. Information such as tree species and amount of water used by different trees was unable to be considered when developing the guidelines, due to the lack of adequate data. Consequently, footings are either being under-designed, which adds to the risks of footing failure, or overdesigned,

leading to increased construction costs. This study closely monitored the water use of a tree in a row of large Australian native eucalypts, *C. maculata*, using a sap flow sensor. The field measurement data were then employed to evaluate the effect of this tree on soil movement and changes in soil suction and moisture content.

2 Field site description

An experimental site located about 28 km southeast of the CBD of Melbourne, Australia, was established in September 2017 for monitoring ground movements, variations in soil moisture and suction, and water use of a large *C. maculata*. The site elevation was 80 m, and the site was located in Climate Zone 3 [22, 35], which is characterized by mild to warm summers and cool to cold winters. The study area is covered with deposits of Quaternary aged alluvium (Qra), containing grey or yellowish-brown duplex soils. According to 71 years of meteorological data, the average yearly temperature ranged from 9.4 to 20.3 °C [5]. The mean annual solar radiation and precipitation were 15 MJ/m² and 859 mm, respectively. A row of five *C. maculata* with an average height of 17.8 m is located in close proximity to an access road to a park (Fig. 2). A tree from this row was selected and installed with a sap flow sensor, which was protected by a steel cage with a protective shade cloth cover to minimize direct sunlight on the



Fig. 2 The selected tree within a row of *C. maculata* trees growing in a suburb of Melbourne

sensor. The chosen tree has a height and crown height of 17.0 m and 10.8 m, respectively, measured using a digital clinometer. The crown diameter of 11.9 m and canopy area of 51.6 m² were determined following the photogrammetry method introduced by Sun et al. [37]. The leaf area index (LAI) of 1.82 was measured beneath the canopy using a Digital Plant Canopy Imager CI-110.

3 Site establishment and instrumentation

Various instruments were deployed at the field site in the early spring months of 2017, including ground surface and sub-ground probes, aluminium access tubes, in situ soil hygrometers, a sap flow sensor and associated power supply system. The locations of monitoring points relative to the *C. maculata* are presented in Fig. 3.

3.1 Ground movement probes

To assess the impact of tree roots on surface and sub-surface soil movements, four surface movement probes were positioned at 4.6 m, 7.8 m, 10.0 m and 14.2 m from the tree trunk, while the 0.5 m and 1.0 m sub-surface movement probes were installed at 6.2 m and 8.6 m from the tree. The surface pad consisted of a 110 mm long × 25 mm diameter galvanized steel bar fixed to the centre of a 100 mm (high) by 100 mm (diameter) concrete block. The sub-surface probe consisted of a 50 mm (high) × 75 mm (diameter) cylinder-shaped concrete base with a 0.5–1.0-m-long, 25-mm-diameter galvanized steel rod embedded in the centre of the concrete base. During the field installation, PVC pipes were inserted into pre-drilled 100-mm-diameter holes with depths of 0.5 m and 1.0 m, and the sub-surface movement probes were inserted all the way to the bottom of the hole. A 90-mm-diameter PVC cap was used at the top of the PVC pipe to prevent the ingress of rainwater.

3.2 Soil hygrometers

To measure total soil suction in proximity to the *C. maculata* tree, three in situ soil hygrometers (Wescor PST-55) were installed at depths of 0.9 m, 1.8 m and 2.5 m at a radial distance of 7.0 m from the tree trunk (Fig. 4). The top of the bore casing protecting the hygrometers was sleeved with a 300-mm-long, 150-mm-diameter PVC pipe and capped with a 150-mm-internal-diameter cast iron cover to prevent rainwater and vandalism. Soil water potential measurement was based on the establishment of water vapour pressure equilibrium between the soil moisture and the air above the soil under isothermal conditions. The Wescor PSYPRO was used to take dew point readings

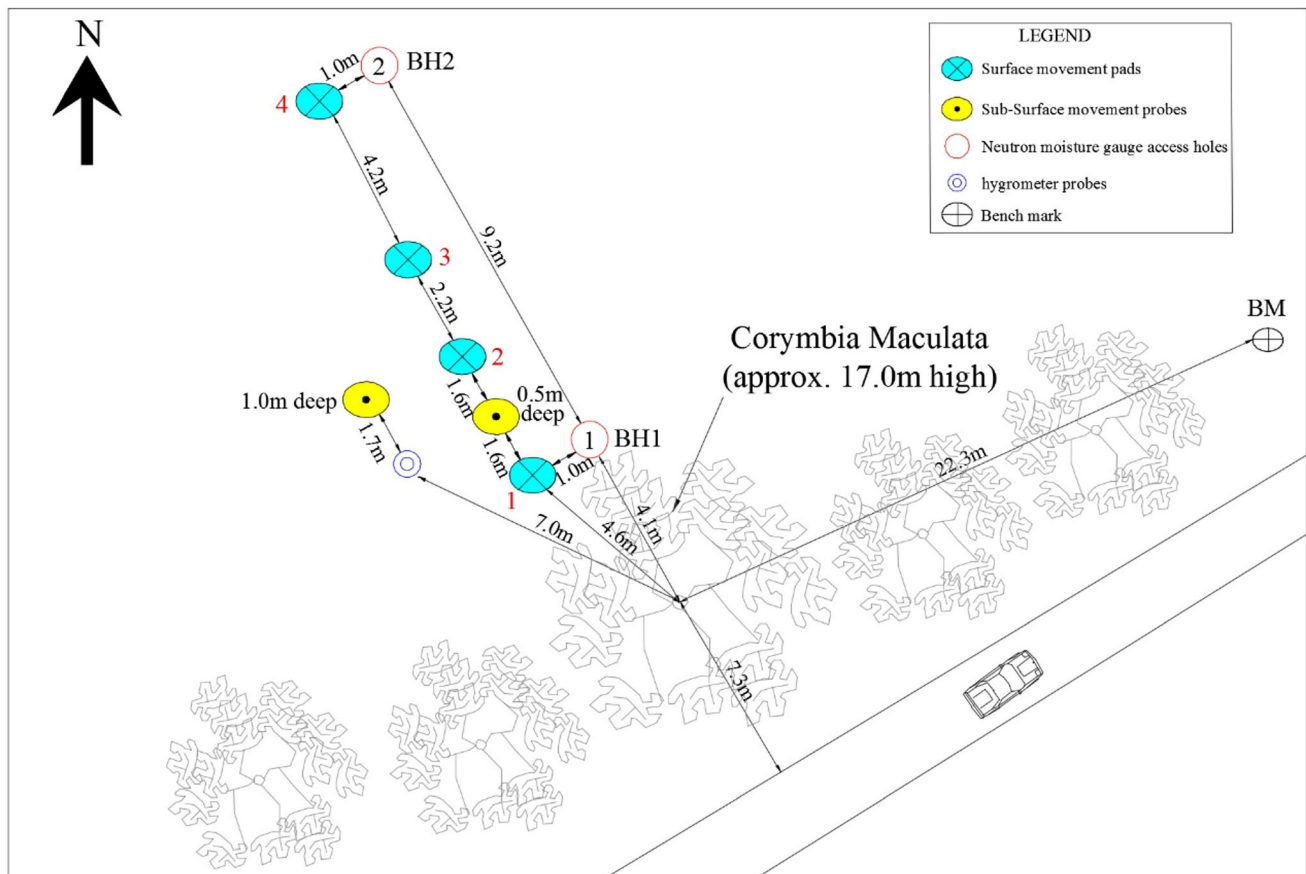


Fig. 3 Location of the *C. maculata* tree and monitoring instruments at the field site in a suburb of Melbourne (not to scale)



Fig. 4 Wescor PST-55 soil hygrometers

by plugging hygrometers into the ports in the control board. All hygrometers were calibrated in a sealed container

containing three layers of filter papers wetted with sodium chloride (NaCl) solution at different concentrations in a customized water bath box and covered the anticipated range of the total soil suction at the field site.

3.3 Neutron moisture meter and access tubes

Soil moisture measurements were taken using a neutron moisture meter (NMM) because of its ability to reach greater depth in the soil profile in a non-destructive way. The wide measurement range also allows its use across large study areas [11, 24, 25]. This study measured the soil volumetric moisture content at two different locations from the tree using an NMM (Campbell Model 503DR). The NMM (Fig. 5) consists of a probe attached by cable to a counting device placed in a shielded casing. The probe includes a radioactive source emitting fast neutrons which collide with hydrogen atoms in the soil and a detector receiving the number of thermalized neutrons. The number of thermalized neutrons moving back to the detector correlates with the water content in the soil. According to CPN International [10], the measurement precision is proportional to the square of the count, so greater precision will



Fig. 5 Neutron moisture meter (Campbell Model 503DR) used to determine soil moisture levels in the vicinity of a *C. maculata* tree

be achieved by releasing a large number of high-energy neutrons from the probe and by longer count durations. Li et al. [24] found that 16 s neutron counts can yield sufficiently precise readings compared to 32, 64 and 256 s counts. The neutron count is not commonly employed in developing the calibration curve due to potential shifts in the source and electronics; instead, the neutron count ratio (NCR) has been adopted by researchers [19]. The NCR is obtained by using the neutron count measured in the soil divided by the standard count measured in the shielded casing of the probe.

In the field site, two 50-mm-diameter NMM aluminium access tubes were installed into pre-drilled holes with depths of 3.9 m at the dripline (4.1 m away from the tree) and at 13.3 m away from the tree trunk, respectively. The gap between the tube and the soil wall was backfilled with soil from the same borehole. The top end of each tube was secured with a cast iron cover, while the bottom end was sealed. The silty clay soil samples obtained during the installation were collected and transported to the laboratory for volumetric water content determination, and the NMM readings were taken shortly after. The calibration curve (Fig. 6) consisting of 8 data points was developed by relating the NCR at pre-determined depths using the NMM to the measured volumetric water content at the same depths using Eq. 3. Calibration coefficients of -60.14 and 69.64 were determined.

$$\theta_v = A \times \text{NCR} + B \quad (3)$$

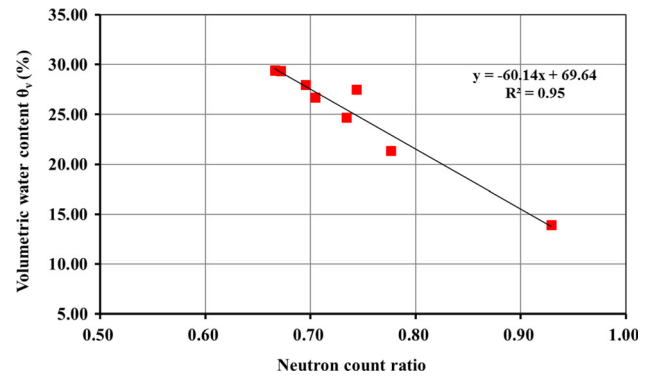


Fig. 6 Calibration curve of the neutron moisture meter (NMM) used to determine soil moisture content

where θ_v is the volumetric water content measured in the laboratory and A and B are calibration coefficients obtained from the regression line.

3.4 Dewpoint potentiometer WP4

Researchers have used the dewpoint potentiometer WP4 (Decagon Devices, Inc., Pullman, USA) to measure total soil suction and leaf water potential [27, 34, 38] as it provides a fast, accurate and reliable measurement. The WP4 measures the total water potential using the chilled-mirror dewpoint technique pioneered by Gee et al. [18], which measures the temperature when condensation first appears. The WP4 consists of a housing chamber containing an infrared thermometer, a temperature sensor, a fan, a mirror and a photodetector cell. When performing a suction measurement, a standard steel ring with a diameter of 27.5 mm and a height of 8 mm is used to form the testing specimen and is then placed in the sliding drawer. After the chamber is closed, the sample is raised and the chamber is sealed to commence the measurement procedure by allowing the sample to equilibrate with the humidity in the chamber. Temperature control is essential when operating a WP4 since the temperature can cause variations in relative humidity owing to the temperature dependence of vapour pressure saturation. A large temperature gradient can cause longer equilibration times and inaccurate results [20]. WP4 is periodically calibrated using the solution of potassium chloride.

3.5 Sap flow meter

Sap flow provides a good indication of plant transpiration as ninety-nine per cent of sap flow is lost through transpiration [33]. Sap flow sensors such as sap flow meter SFM1 have been widely used to measure sap flow in trees and to estimate whole plant canopy transpiration due to their low power requirement, reliability and easy

installation [21, 26]. Burgess et al. [6] assessed the accuracy of SFM1 and concluded that it could provide accurate measurements for high, low and reverse sap flow rates in a wide variety of tree species. The SFM1 used to measure sap flow in *C. maculata* in this research consisted of three 1.3-mm-diameter and 35-mm-long measurement needles (one heater needle and two temperature needles) connected to the device (Fig. 7a). Each temperature needle contains two sensors positioned 15 mm apart. The SFM1 is programmed with the heat ratio method (HRM), which measures the temperature of moving sap in the water-conducting xylem tissue following a short pulse of heat applied by a line heater located 6 mm away from the temperature sensors. The internal 4.2 V lithium polymer battery can usually last for three days, depending on weather conditions. To ensure continuous logging of sap flow, the internal battery was directly connected to a customized power supply system consisting of a timer and two batteries with the 12 V outlet placed in a stainless-steel box, as shown in Fig. 7b. The SFM1 was installed on the north side of the *C. maculata* because the highest sap flow rate was found on the north side of trees in the southern hemisphere [38]. When calculating transpiration from the SFM1 data, it was assumed that the tree has a symmetrical cross section and that sap flow was uniform around the circumference.

4 Soil testing

Two 40-mm-diameter boreholes (BHs) were drilled to 4 m deep, at distances of 4.1 m and 13.3 m away from the tree trunk to provide soil samples to establish soil profiles from a series of laboratory tests. Soil profiles are presented, and initial soil moisture contents and suctions, Atterberg limits, shrink–swell indices and an SWCC drying curve are also provided.

4.1 Soil profile

Table 2 presents the soil profile of BH 1. Generally, the soil consisted of fill up to 1.5 m deep, including a topsoil layer 0.15 m thick. The fill was a 1.35-m-thick layer of clayey silt (ML). Intermediate-plasticity silty clay (CI) was observed to a depth of 2.75 m, which became high plasticity to the full depth of the borehole (i.e. 4 m). Fine tree roots or rootlets were observed from 0.25 to 2.75 m, with the diameter varying between 0.15 mm and 0.8 mm. BH 2 has a similar soil profile to BH 1, but with no rootlets observed over the soil profile.

4.2 Initial soil moisture and suction profile

Soil samples from the two BHs were collected at every 0.25 m, wrapped in aluminium foil, stored in plastic bags, and transported to the laboratory to conduct soil moisture

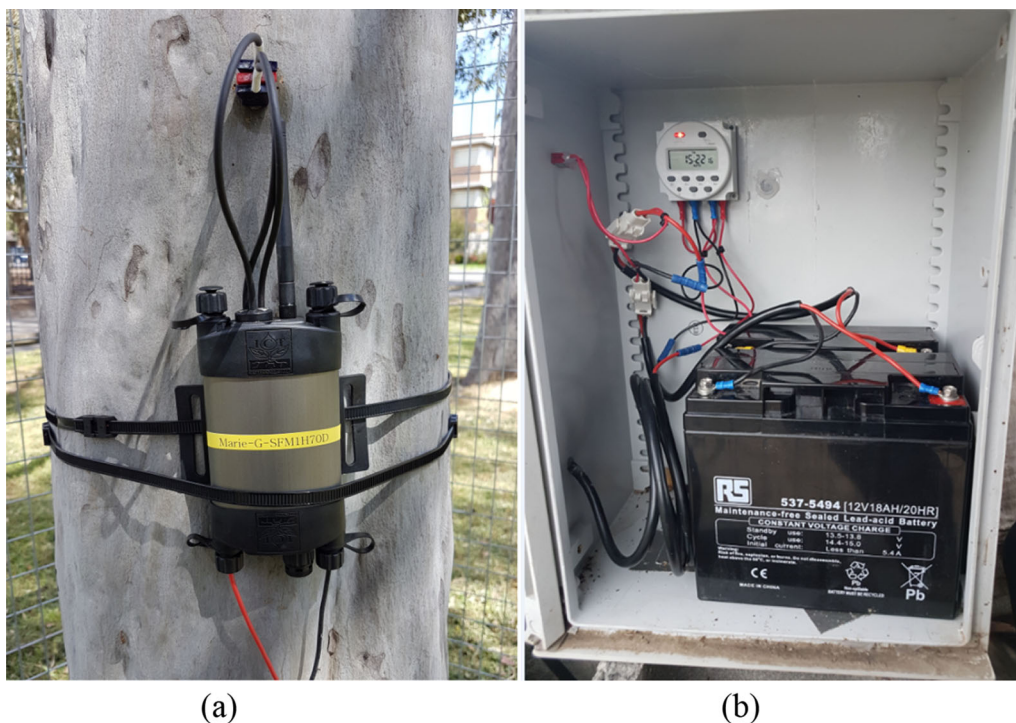


Fig. 7 Sap flow measurement of the *C. maculata* tree at the field site **a** SFM1 and **b** power supply system

Table 2 Soil profile of BH 1 to a depth of 4 m near the *C. maculata* tree

Depth (m)	Description
0.00–0.15	Fill—silt (ML), dark brown, moist
0.15–1.50	Fill—clayey silt (ML), dark greyish brown, mottled dark yellowish brown, moist, very stiff. Tree rootlets present
1.50–2.75	Silty clay (CI), dark yellowish brown, moist, stiff. Tree rootlets present
2.75–3.45	Silty clay (CH), dark yellowish brown, mottled grey, moist, stiff. Tree rootlets present
3.45–4.00	Silty clay (CH), yellowish brown, mottled grey, moist, stiff

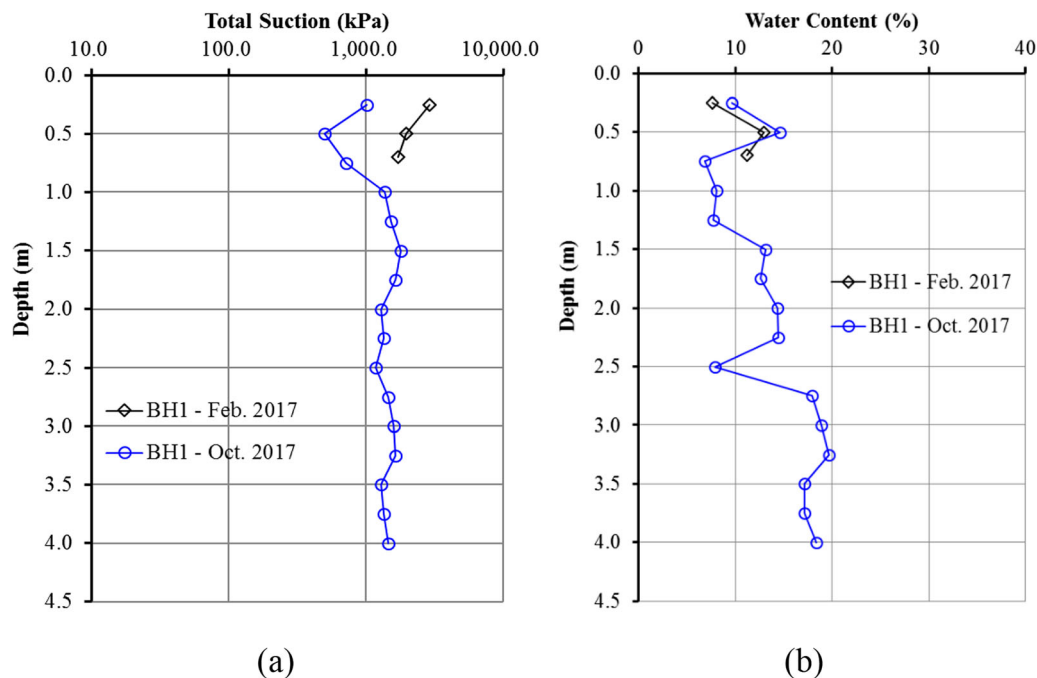
studies. Gravimetric soil water content was measured by weighing the moisture loss before and after oven-drying at 104 °C. Total soil suction was measured with the WP4, and the reported value is the average of three sub-samples.

Figure 8 presents the total soil suction and water content profiles in February and October 2017, respectively, for BH 1 near the *C. maculata* tree. Due to an inability to drive the tube through the fill material for soil sampling in February, the investigation was terminated at a depth of 0.75 m. In February, soil drying over the depth from 0 to 0.75 m was observed from the soil suction profile. A similar trend in February of soil moisture conditions was obtained from the corresponding water content data, revealing a lower

moisture content between the ground surface and 0.5 m deep. This can be explained by the higher evapotranspiration rate near the ground surface in the hotter months. In October, soil suction ranged from 500 to 1790 kPa between the ground surface and 1.75 m and became constant at a value of 1390 kPa below 2.0 m. The rather low moisture content of 7% at a depth of 2.5 m is inconsistent with the suction data and is likely arising from an erroneous reading of mass.

The total soil suction and water content profiles for BH 2 are shown in Fig. 9. Compared to soil sampled in October, high soil suction was observed to a depth of 0.75 m in late summer. The moisture content at 0.75 m depth was higher in February than in October, contrary to the expectation based on the suction at this depth. This is likely caused by the increased osmotic suction primarily affected by soil salinity, which is not reflected by the corresponding soil water content at the same depth. Therefore, the trend of soil suction is more reliable than the patterns of moisture content. At 1.0 m depth, the same soil suction value was measured for both months and this was consistent with the water content measurements. As shown in the soil suction profiles, suction was slightly lower from 2.0 to 3.0 m in February, and a similar trend was obtained from the corresponding water content data.

Soil suction varied from 610 to 1760 kPa in October over the full depth of measurement, while the difference of 890 kPa in suction values was observed in February. Soil suction varied little below 2 m deep in both months, and the suction of 1550 kPa could be considered as the wilting

**Fig. 8** Soil test results for BH 1 near the *C. maculata* tree **a** total soil suction profiles and **b** Water content profiles

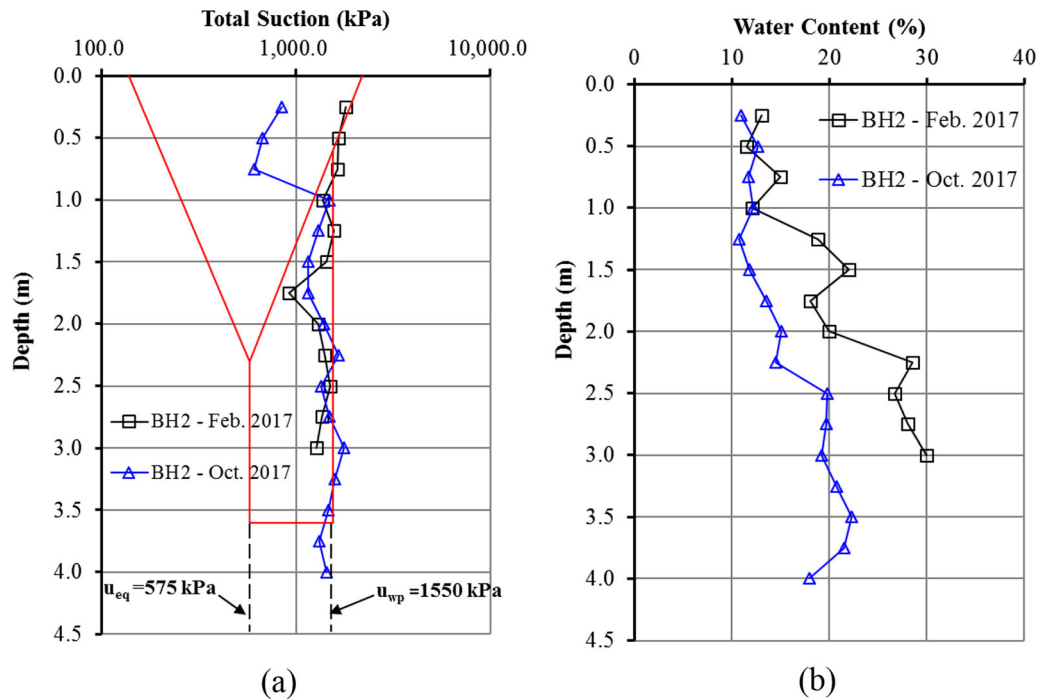


Fig. 9 Soil testing results for BH 2 near the *C. maculata* tree **a** total soil suction profiles and **b** Water content profiles

point suction, 36% lower than the suction of 2431 kPa induced by *Axonopus compressus* and *Cynadon dactylon* [15]. The deep equilibrium suction, u_{eq} of 575 kPa was estimated based on the conservative design value of Δu_{base} of 0.43 pF provided by AS2870 [3]. The climate-induced soil suction profile, the trees-induced extra suction profile based on the estimated values of u_{eq} and u_{wp} , and the suction change profiles are superimposed on the plot in Fig. 9a, revealing that soil suction change from the ground surface to 0.6 m deep was caused by climatic variations, while the change from this depth to at least 3.6 m was caused by root-induced soil drying. The observation that a wilting point suction has been established to at least 4 m deep suggests that soil shrinkage has occurred over the years as the trees grew, well before the monitoring period.

4.3 Atterberg limits tests

The Atterberg limits tests were conducted following AS1289.3.1.2 [1] and AS1289.3.2.1 [2]. The results for soil samples from BH 1 are presented in Fig. 10 and show that the soil at 1.5 m depth can be classified as intermediate-plasticity clay (CI), which becomes high plasticity between 2.75 and 4.0 m. Figure 10b shows that plastic limits ranged from 14 to 20%. The liquid limits varied between 44 and 54% within the top 2.75 m, followed by a notable increase up to 75% at 3 m with a slight decrease to 64% at 4 m. It is noted that the longitudinal soil shrinkage ranged between 9.6% at 2.75 m and 19.1% a further 0.25 m deeper at 3 m.

The testing results also showed that soil from BH 1 is moderate to very high expansive clay. Soils from BH 2 have similar properties to BH 1, with intermediate-plasticity clay (CI) encountered at 1.3 m.

4.4 Shrink–swell tests

Soil samples for shrink–swell tests were obtained at a location 0.5 m away from BH1 by driving 450-mm-long and 50-mm-diameter thin-walled stainless-steel tubes to depths of 0.8 m and 1.7 m using a pneumatic hammer. The soil cores were extruded out of the steel tube using a hydraulic jack after being transported to the laboratory. The shrink–swell test consists of a simplified core shrinkage test and a swelling test, requiring soil samples to have the same initial moisture content. A sample core length that is 1.5 to 2 times longer than the diameter is required for the core shrinkage test. Drawing pins were attached to the two ends and the centre of two sides of the specimen, enabling the measurements of length and diameter changes at different stages of the test. The core sample was wrapped with a plastic membrane overnight on the first day to reduce the risk of cracking followed by air drying for 12 days. The changes in sample diameter and length were recorded at least twice a day using a digital Vernier calliper, while the sample mass was measured by a two decimal point balance. Once changes in sample length and diameter were less than 0.1 mm over the previous 24 h, the sample was oven-dried at 105 °C for 24 h to a constant mass. Figure 11

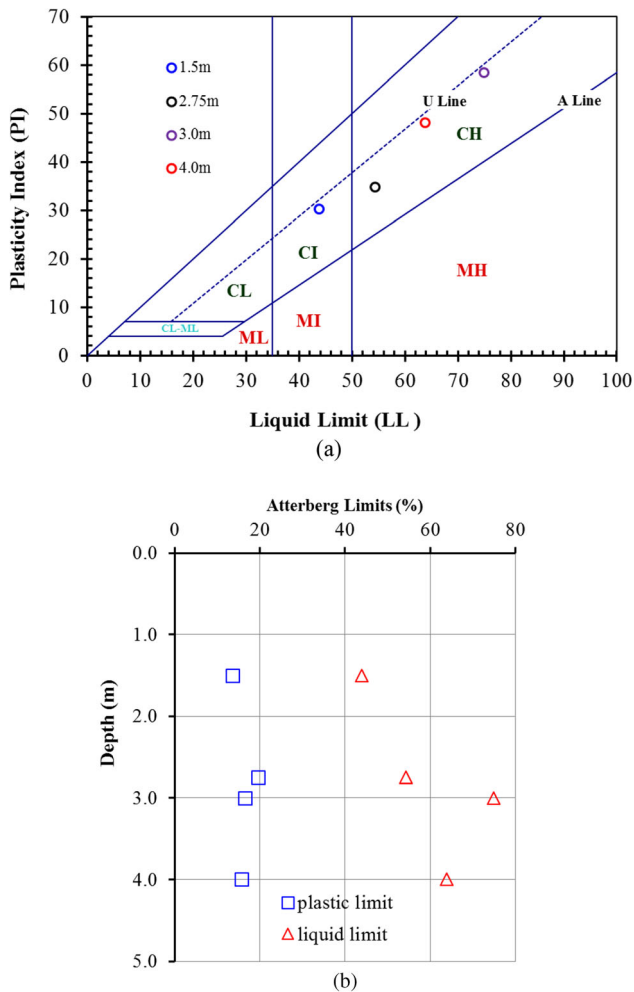


Fig. 10 Atterberg limits test results from BH 1 near the *C. maculata* tree **a** plasticity chart and **b** plastic limit and liquid limit

presents the comparison of axial shrinkage strain, radial shrinkage strain and volumetric shrinkage strain for the sample at 1.7 m depth, showing that the radial shrinkage strain, on average, is 0.3% larger than the axial shrinkage strain at various water contents. The volumetric shrinkage strain of 1.7% was obtained after oven-drying, which is 3.4 times higher than the corresponding axial shrinkage strain.

For the swelling test, the soil sample was cut using a steel ring (20 mm high and 45 mm diameter) and then the ends were trimmed flat. Both ends of the sample were attached to a porous stone plate and then positioned in a consolidation cell. A 5 kPa seating pressure was exerted on the sample for 10 min, and then, the vertical pressure was increased to 25 kPa for a maximum of 30 min. The sample height at the end of the loading period was taken as the datum from which swelling strain was determined. Deionized water was then added to the cell to observe soil swell. The testing was ceased when the swelling increment was less than 1% of the total swelling. An extension ring

(5 mm high and 45 mm diameter) was positioned on the top of the swelling ring to prevent the top of the sample from swelling unrestrained and potentially being eroded.

Results of the swelling test for the soil sample from 1.7 m depth are depicted in Fig. 12. Initial soil settlement was clearly observed in the first 30 min due to the applied pressure of 25 kPa. It is worth mentioning that 79% of the total swelling strain was completed in the first 32 h. A shrink–swell index, I_{ss} of 1.7%/pF was calculated for soil from 0.8 m and 0.5%/pF for soil from 1.7 m. The characteristic soil movement y_s of 19 mm was calculated based on Eq. 1, and a slightly reactive (S) site was determined.

4.5 Soil water characteristic curve

The soil–water characteristic curve (SWCC) expresses the correlation between soil suction and the degree of saturation for unsaturated soils. Figure 13 presents the SWCC drying curve developed for samples at 0.8 m depth. The samples were obtained from the BH that was used to install hygrometer probes. The data points before 1500 kPa were determined using Fredlund SWC-150, which allows the matric suction to be regulated from 0 to 1500 kPa. The suction degree of saturation point beyond 1500 kPa was determined using WP4 following drying in a vacuum desiccator over a salt solution for a month. It is noted that the constraints of 0 kPa and 1,000,000 kPa were assumed. The measurement points were fitted with the best-fit SWCC equation pioneered by Fredlund and Xing [14].

5 Results and discussion

5.1 Soil movements

A Spectra laser level was used to conduct soil surface and sub-surface movements measurement every three weeks. Soil levels were measured against the reduced level of the benchmark, which was located 22.3 m north-east of the tree. Soil movements were calculated based on the initial level measured during October 2017. Negative soil movements indicate settlement, while positive movements express heave. The distances of surface pads and sub-surface probes to the tree are presented in Fig. 3. It is noted that all pads, probes and BM for conducting the level survey were removed in November 2018 by the Knox City Council due to capital works.

Level survey data in close proximity to the *C. maculata* from October 2017 to October 2018 are presented in Fig. 14. As previously discussed, soil movements had occurred prior to the level surveys, as evidenced by the soil suction data and the establishment of a deep wilting point suction. The following observations relate to movements

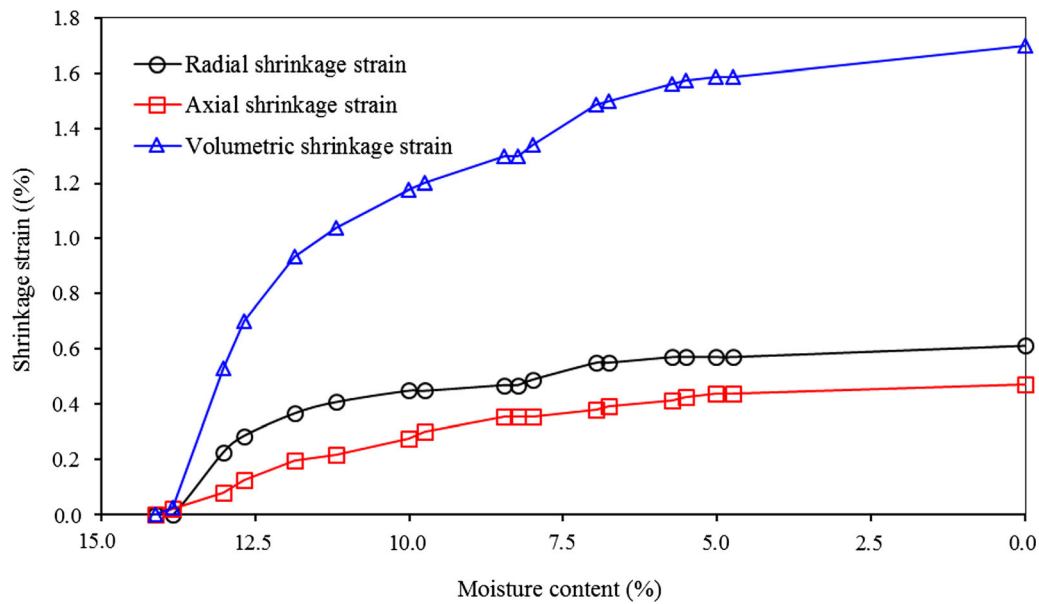


Fig. 11 Comparison of axial shrinkage strain, radial shrinkage strain and volumetric shrinkage strain for the soil sample obtained at 1.7 m depth near the *C. maculata* tree

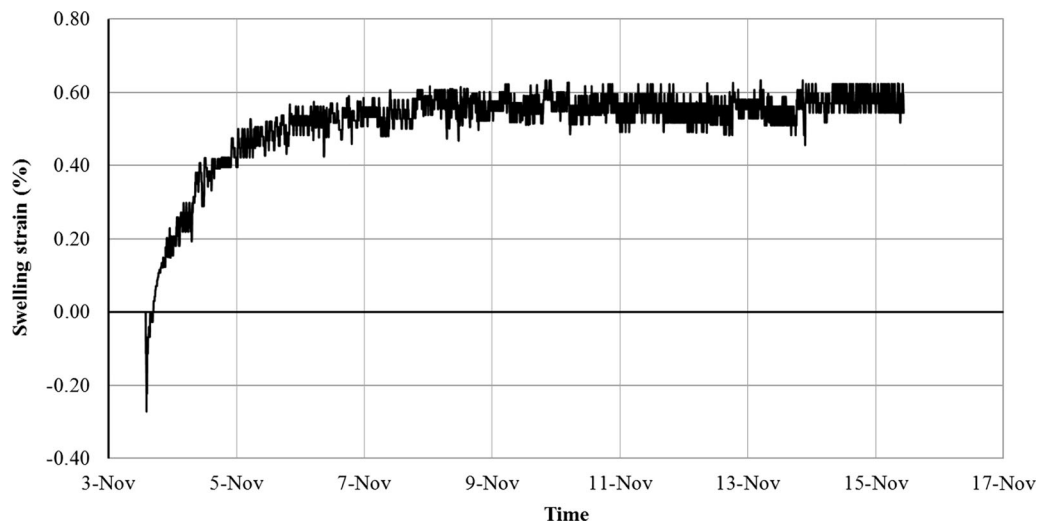


Fig. 12 The soil swelling strain versus time for the sample at 1.7 m depth near the *C. maculata* tree

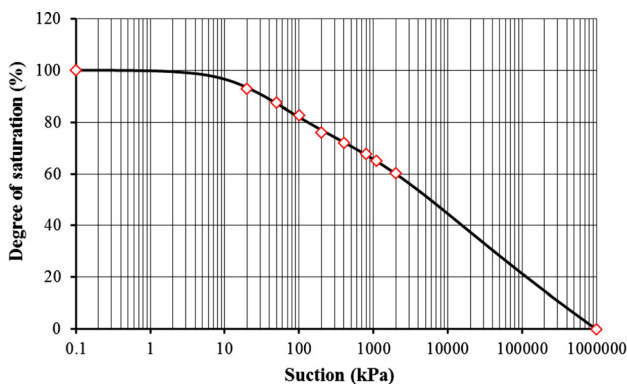


Fig. 13 The SWCC drying curve for soil from 0.8 m depth

within the monitoring period. Surface soil at a distance 7.8 m away from the tree (i.e. surface pad (2), $D: HT = 0.5$) experienced the greatest shrinkage settlement of 11 mm compared to soil further from the tree. A significant soil heave was observed for almost all the monitoring points (except surface pad (2)) from mid- to late autumn 2018, with the maximum heave of 10.0 mm occurring at distances of 6.2 m and 14.2 m from the tree trunk. It is noted that surface pad (2) experienced negative movements from November 2017 to August 2018, while continuous heave was observed for surface pad (4) over the monitoring period. A similar but smaller settlement of 5 mm was recorded for surface and sub-surface soils except for

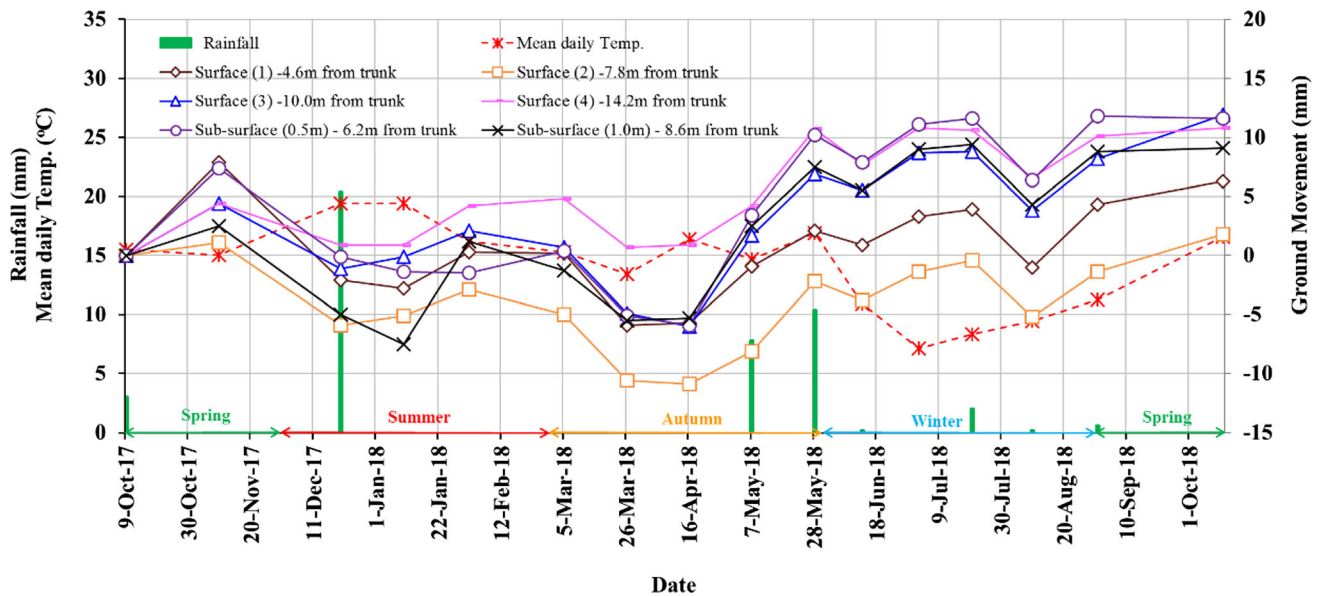


Fig. 14 Surface and sub-surface soil movement and rainfall and mean daily temperature from October 2017 to October 2018 near the *C. maculata* tree

surface soil at 7.8 m and 14.2 m away from the tree, when the level survey was conducted in March and April 2018. A relatively smaller movement occurred from winter to mid-spring 2018 for all the monitoring points. It is important to note that the ground movement due to variation in soil moisture content and suction is partly impacted by tree water uptake; other factors such as soil type, climate (air temperature, precipitation and evapotranspiration) and topography could also affect soil water dynamics. Two meteorological parameters, including rainfall and mean daily temperature, which is calculated by averaging the daily maximum and minimum temperature, are also plotted in Fig. 14 to see whether there were any correlations with soil movements. No direct relationship was found between soil movements and these two weather parameters. However, an indirect relationship is expected between rainfall and ground movement. It takes time for rainwater to percolate to deeper soil layers following a precipitation event, leading to delayed increases in soil water content and subsequent soil heave at these depths. In contrast, rainfall water can easily enter deeper soil layers if large cracks develop on the surface in hotter months, although this was not observed during the monitoring period. A combination of higher temperatures and frequent rainfall events is also predicted to influence soil movement. For example, soil subjected to an initial shrinkage settlement when the temperature is high in summer and autumn may experience a substantial heave under the effect of more frequent rainfall events in winter and spring.

5.2 Soil moisture content

Soil volumetric water content measurement was taken by NMM at a distance of 4.1 m (NP1) and 13.3 m (NP2) from a tree within a row of trees. The duration for emitting and detecting neutrons was selected as 16 s; however, measurements were taken twice at each stopping point, and the average neutron count was adopted to represent the moisture level. The profiles of soil volumetric water content presented in Fig. 15 depict count ratios from October 2017 to May 2021 for NP1 and NP2, respectively. The lower and upper envelope of all measurements taken over the study period is shown. A significant variation in volumetric water content occurred within the top 1.1 m for NP1, which lessened below this depth until 2.2 m was reached. The water content remained almost constant from 2.2 m to the full depth of 3.6 m. Soil drying was evident between 0.6 and 1.2 m since the lowest water content of only 10% was measured during mid-summer of 2021. High soil water content was observed from 2.2 m to the full measurement depth.

As presented in Fig. 15, a relatively smaller change of water content occurred from 0.4 to 1.1 m for NP2 compared to water content variation over the same depth for NP1. The seasonally wetter soil over this depth at NP1 is possibly due to the large tree canopy, which shades the soil and thus prevents its surface from excessive and rapid drying. The soil was relatively drier within the top 0.7 m for NP2 than the soil over the same depth close to the dripline. Similar to NP1, an increase in soil water content was found from 2.2 to 3.9 m for NP2. It was noticed that

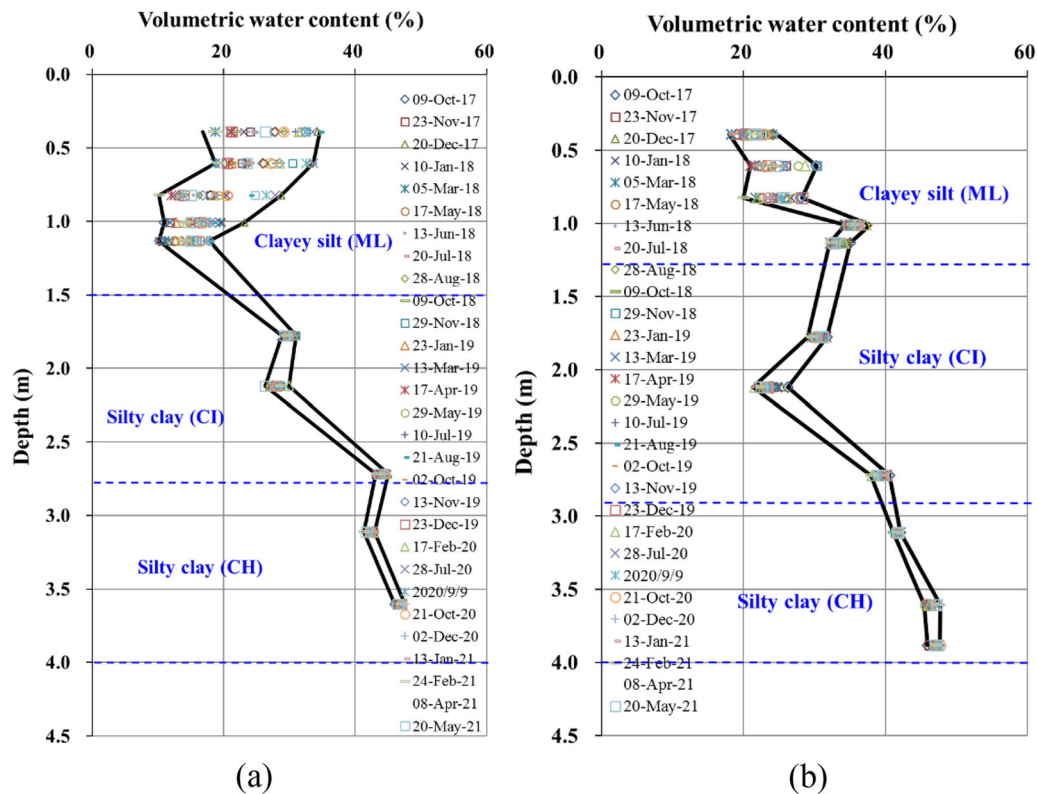


Fig. 15 Soil volumetric water content profiles near the *C. maculata* tree **a** NP1 and **b** NP2

soil water content varied only slightly below 2.2 m for both locations.

The soil volumetric water content profiles showed that the additional drying effect of tree roots probably lay between 0.6 and 1.2 m depth as volumetric water content varied from 10 to 34% over these depths, significantly lower than soil water content further from the tree. Generally, the soil water content variations for both locations exhibited a similar trend. The variation of soil water content range decreased with depth, with significant changes occurring within the top 1.0 m for both NP1 and NP2. An increase in volumetric water content occurred from 1.2 m down for NP1, while an opposite trend was observed for NP2, although water content remained at approximately 30% for the two locations at 1.75 m. The volumetric water content is greater than 40% for soil below 2.8 m for both locations.

Figure 16 shows a comparison of the variations in volumetric soil water content from January to July 2018 from a depth of 0.4 m and below for NP1 and NP2. The maximum soil differential movements close to the dripline (pad 1, 4.6 m away from the tree) and 14.2 m (pad 4) away from the tree over the same period were determined. The surface pads 1 and 4 were located one metre away from the soil water content measurement points, NP1 and NP2, respectively (Fig. 3). The soil in close proximity to the tree

experienced a maximum differential movement of 6.7 mm due to notable changes in soil water content within the top 1.8 m over 7 months. An increase in soil water content of 5.8% was observed at a depth of 1.2 m, from 10.2% in January to 16% in July. The low water content in January is most likely caused by the drying effect of tree roots in summer (Fig. 16a). In contrast, there is no indication of tree-induced soil drying for NP2, although a maximum of 5.2% change in water content was observed at 0.4 m depth (Fig. 16b). A maximum differential movement of 9.7 mm during the study period was considered as an effect of climatic variations.

5.3 Soil suction

The in situ soil suction profiles for the measurement period from October 2017 to June 2021 are shown in Fig. 17. The location of these measurements as shown in Fig. 3 is about 3 m to the side of NP1. An envelope showing the range of highest and lowest total suction values for all measurements is indicated. As shown in Fig. 17, the greatest variation of soil suction of 50–1620 kPa occurred at 0.4 m depth, although most of the measured suction values were smaller than 300 kPa. This is consistent with the soil volumetric water content measured by NMM, revealing that the soil near the ground surface had experienced more

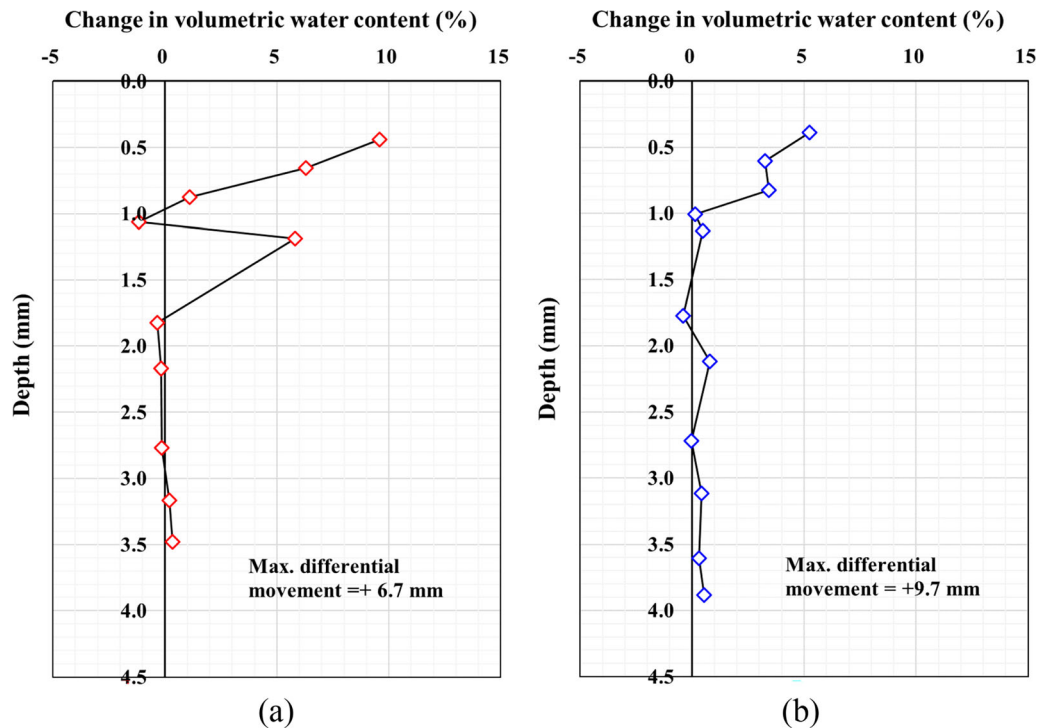


Fig. 16 Changes in volumetric water content from January to July 2018 **a** NP1 and **b** NP2

significant water content variation. The suction variation narrowed at a depth of 0.9 m, ranging from 680 to 1340 kPa, with the corresponding volumetric water content varying between 11 and 24%. The inferred u_{wp} aligns well with the high suction limit.

The seasonal variations of soil suction at various depths near the tree's dripline are depicted in Fig. 18. Generally speaking, a substantial rise of soil suction was observed in hotter, drier months (i.e. summer and autumn) for soil suction measurements at all depths during the monitoring period. It was observed that the highest suction in the season cycles was 1900 kPa, 1580 kPa and 1740 kPa, which occurred at 1.8 m depth in early winter for the first season cycle, in late winter for the third season cycle and in early autumn for the fourth season cycle, respectively. It should be noted that soil suction measurements ceased from March to July during the third season cycle due to the COVID-19 pandemic and subsequent lockdowns. For the second season cycle, the maximum suction of 1770 kPa occurred at 2.5 m in late autumn. It is noted that the soil suction of 1520 kPa obtained for a depth of 2.5 m in February 2019 was exactly the same as the suction value measured during the initial investigation for the same depth in February 2017.

Two meteorological parameters, namely rainfall and mean daily temperature, are also plotted in Fig. 18 to see whether there were any correlations with suction measurements. It was found that rainwater can lead to a

decrease in soil suction close to the ground surface (e.g. 0.4 m), although no significant impact was observed for deeper soils below 1.8 m. The high air temperature could substantially increase the suction at all depths in summer and autumn.

5.4 Leaf water potential

The WP4 was used to measure the leaf water potential of the *C. maculata* tree. Three leaf samples were removed at the petiole junction from different tree branches for water potential measurement and the average value is reported. The seasonal variation pattern of leaf water potential for *C. maculata* from July 2018 to May 2021 is presented in Fig. 19. Figure 19 also includes a plot of the soil suction measurements taken at various depths during the same period for comparison. It should be noted that the breaks for soil suction at a depth of 0.4 m over the monitoring period are due to soil that was too wet, exceeding the measurement range of the Wescor PSYPRO instrument. It is evident that the leaf water potential varied greatly from summer to winter, with the maximum water potential of 6.48 MPa occurring in early summer in 2020 and the minimum water potential of 3.10 MPa occurring in mid-winter in 2019, respectively. The maximum leaf water potential of the tree is significantly higher than the inferred wilting point soil suction u_{wp} of 1.55 MPa for the site, although it was stated by Cameron and Beal [9] that the

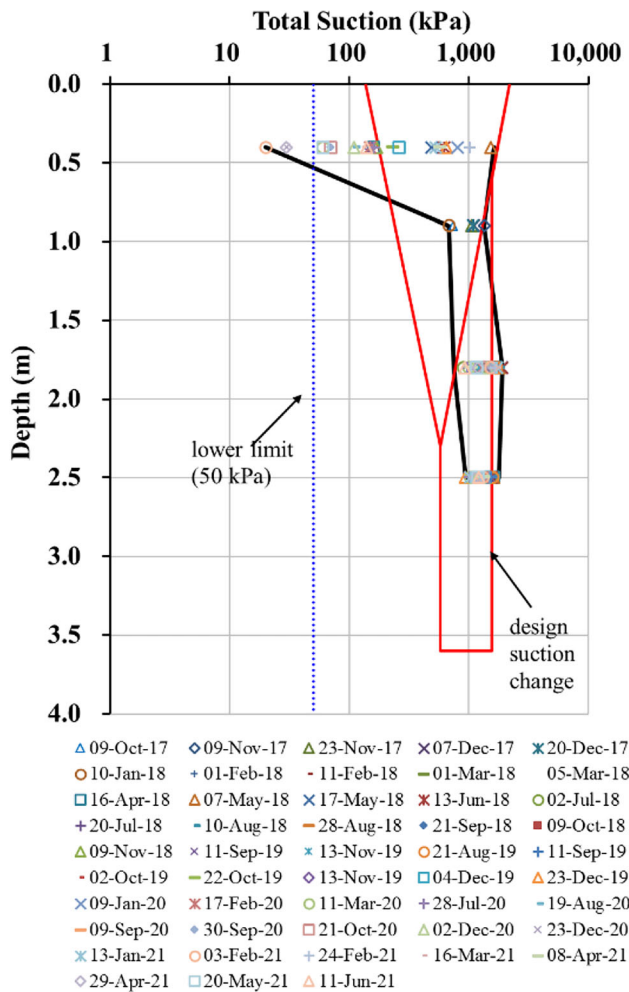


Fig. 17 Soil suction profiles close to the dripline of the *C. maculata* tree

maximum leaf water potential can be conventionally taken as an estimation of the corresponding wilting point soil suction. An average leaf suction of 4.71 MPa was calculated over the monitoring period. A gradual decrease of leaf water potential was observed from early autumn through to winter for all the season cycles over the monitoring period. Figure 19 clearly reveals that the leaf water potential of the tree is significantly higher than the soil suction at all depths; this explains why tree roots can draw water from the soil. Soil suction and leaf water potential exhibited a dissimilar variation trend; this could be attributed to the fact that the changes in leaf water potential are governed by seasonal and diurnal variations, while the suction change in clay soils does not occur instantaneously.

5.5 Tree sap flow

The sap flow data were measured at 30-min intervals using SFM1. The sap flow patterns were compared with maximum temperature and solar radiation over 31 days in January 2019, as shown in Fig. 20. Generally, the daily sap flow presents a bell-shaped curve, with the highest flow rate developed in the afternoon and then progressively descended, stabilizing around zero flow at midnight. Fairly similar sap flow patterns for individual trees are found in many studies [12, 26, 29, 36, 37].

The low rate of sap flow that occurred on 18 January (Fig. 20) is attributed to the low daily solar radiation of 5.9 MJ/m². A noticeable decline in sap flow on 24 and 25 January is most likely due to early stomatal closure as a result of the scorching daily temperatures exceeding 40 °C. Significant nocturnal water uptake was observed the following day, contributing 9% of the daily total sap flow

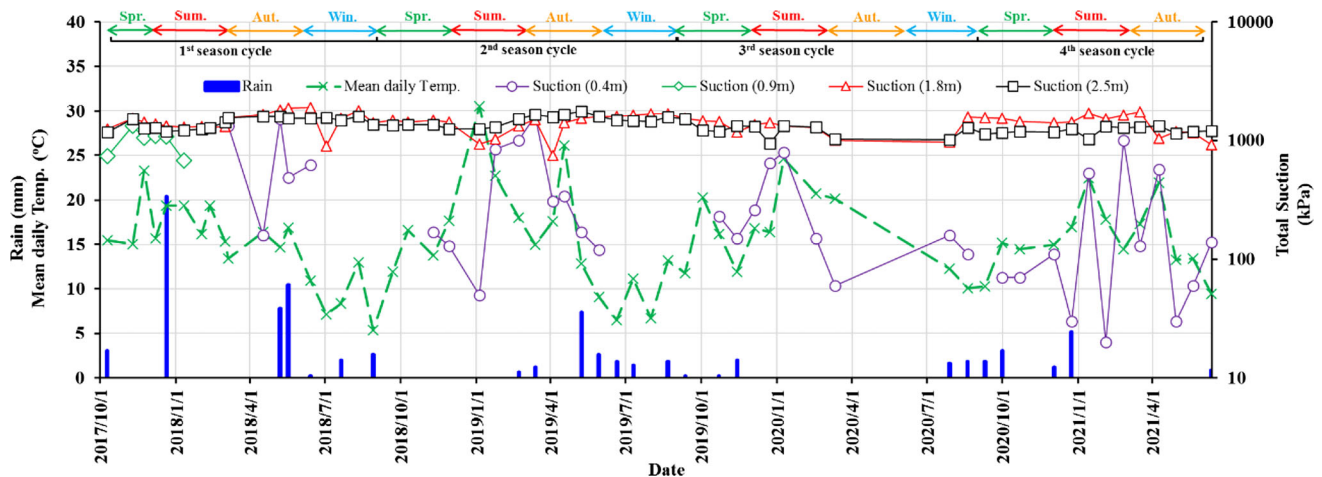


Fig. 18 Variation in soil suction close to the dripline of the *C. maculata* tree

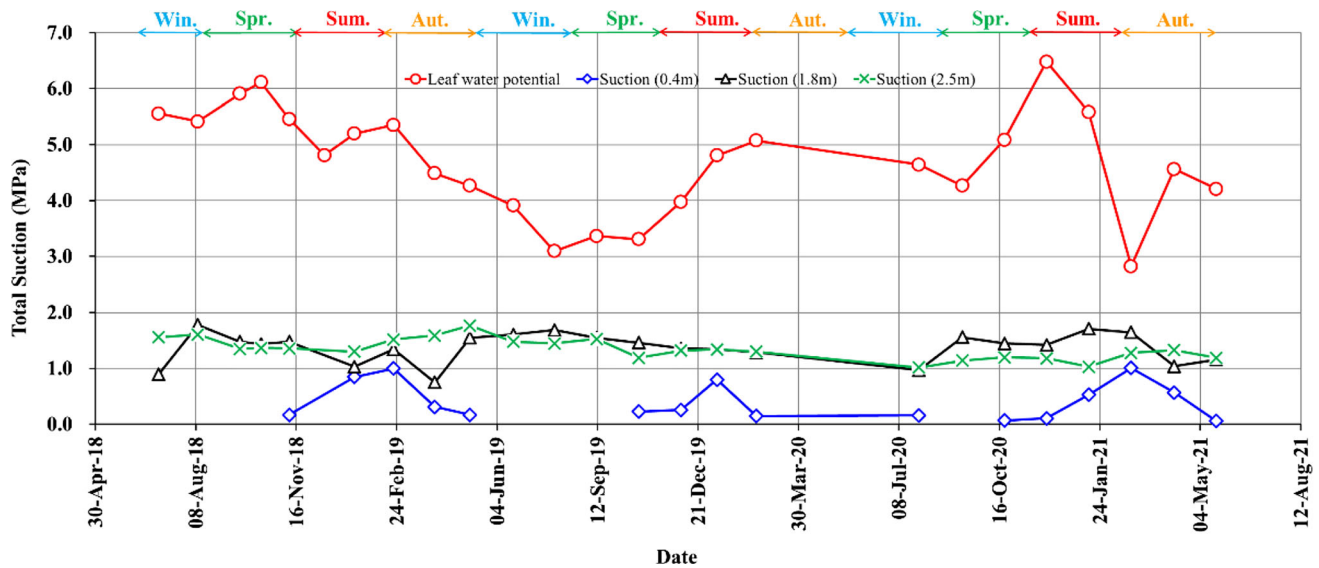


Fig. 19 Comparison of soil suction at different depths with leaf water potential (expressed as suction) for the *C. maculata* tree

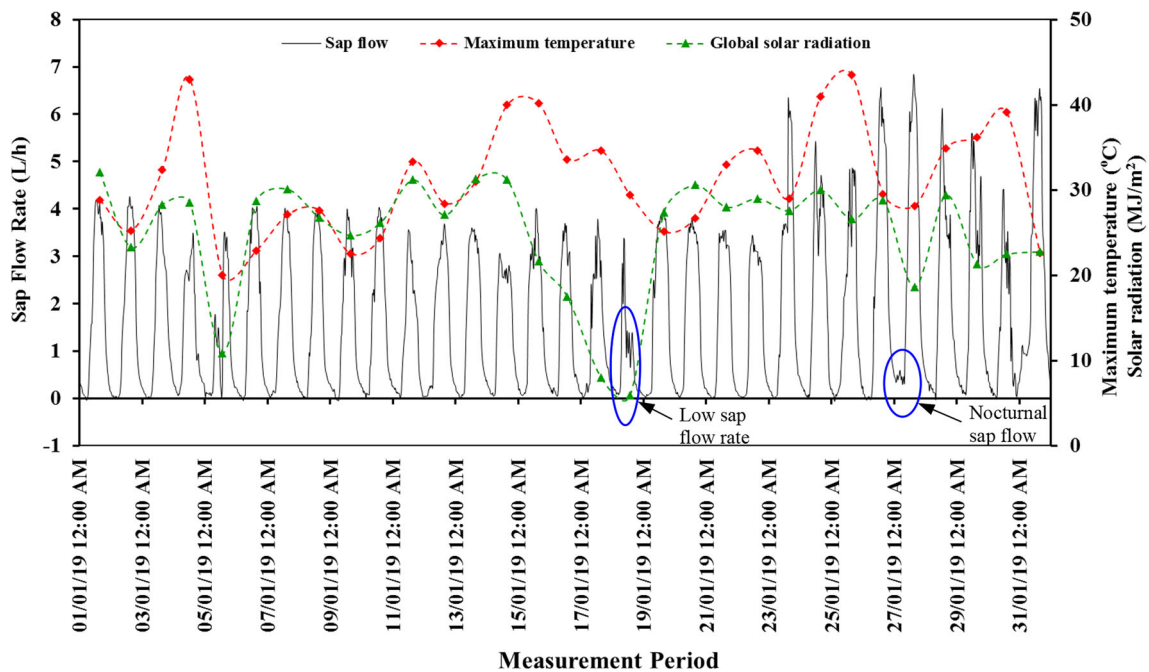


Fig. 20 Comparison of the trend of sap flow in the *C. maculata* tree with temperature and solar radiation in January 2019

volume. This value is similar to the study conducted by Loustau et al. [28], who found nocturnal sap flow constituted 12% of the daily total transpiration.

Monthly sap flow volume for *C. maculata* was compared from September 2017 to May 2021, as shown in Fig. 21. Very similar trends of variation of monthly sap flow volume were observed for each year, despite significant variations in daily water use. Generally, this tree had its greatest water demand in summer with a maximum sap flow rate occurring in January. The transpiration rate

decreased in winter months, with the lowest water use occurring in June and July. The water use of this 17 m high tree exceeded 2 kL in December 2017 and January 2018, which is significantly less than the water use of 5.9 kL in January for a 14.6 m tall single tree from the same species [38]. The lowest monthly water use occurred in May 2021, with a mean daily transpiration of only 10.3 L. It is evident that transpiration from September to December in 2017 was higher compared to the same month in other years. The transpiration of 2.06 kL in December 2017 is 49% higher

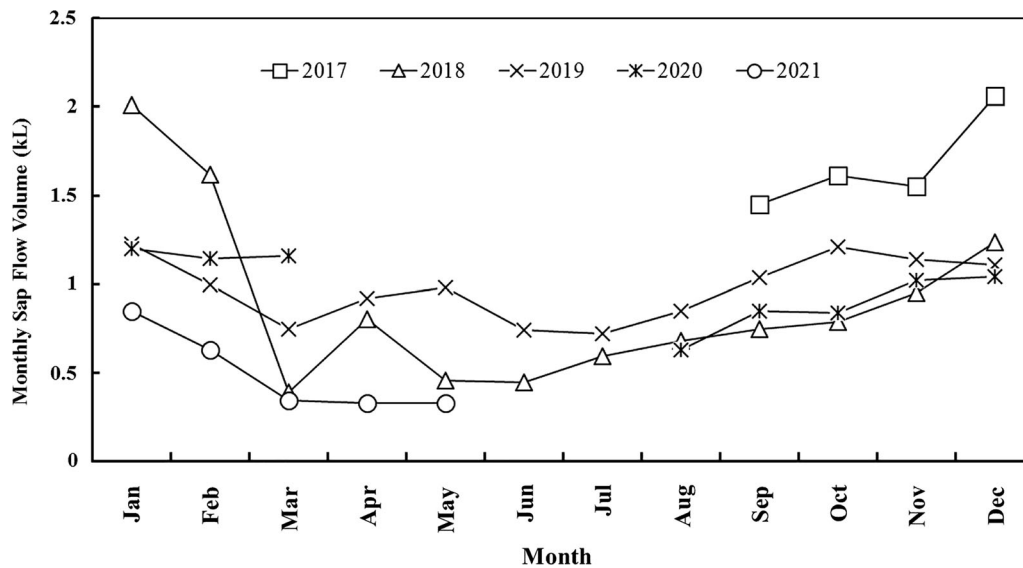


Fig. 21 Comparison of monthly sap flow volume for the *C. maculata* tree from 2017 to 2021

than the water use of 1.04 kL for the same month in 2020, most likely due to the more frequent rainfall events in December 2017 contributing to a monthly total of 164 mm, which is 68% higher than the total rainfall in December 2020.

6 Conclusions

A fully instrumented site with a large tree within a row of native *C. maculata* trees in the eastern suburb of Melbourne, Australia, was closely monitored for sap flow and nearby soil movement; soil moisture and soil suction were measured regularly over a period of 44 months.

The level survey conducted in the vicinity of and well away from the selected tree showed that soil shrinkage settlement partly caused by root-induced soil drying during the period of monitoring was significant at 7.8 m away from the tree ($D: HT = 0.5$); however, the settlement became smaller as the ground is away from the tree, with no tree-induced soil settlement observed at 14.2 m away from the tree ($D: HT = 0.8$). The soil volumetric water content profiles based on NMM data for NP2 ($D: HT = 0.8$) also show no apparent water content decrease caused by root-induced soil drying. The proximity ratio of 0.8 could be considered a safe distance in terms of the foundation design, 47% smaller than the conservative ratio of 1.5 provided by the Australian Standard. This means that over-design a footing could be avoided, and thus, a

significant cut on footing construction cost if the proximity ratio determined by this study is adopted. The maximum tree root drying depth was determined to be 1.2 m from the volumetric water content profiles for NP1 ($D: HT = 0.2$), which revealed soil drying between 0.6 and 1.2 m, likely caused by the drying effect of tree roots near the dripline during hotter months. The study concludes that the influence of root-induced soil drying varied from 4.1 m ($0.2 HT$) to 14.2 m ($0.8 HT$), while the depth of influence reached 1.2 m. Relatively low soil movements during the study period can be explained by the inferred wilting point suction in Fig. 9 and the upper suction boundary established in Fig. 17, suggesting the deeper shrinkage settlement has been established at the site prior to monitoring, while the monitoring period mainly showed the effects of shallow drying. Both are needed to prevent any footing movements that could arise from the planting and removal of new trees around light buildings.

More studies on safe distance for footing design for a single or a group of different tree species are desperately needed to improve the current footing guidelines and promote a higher level of understanding of tree-induced soil desiccation. Researchers could utilize the long-term field measurement data presented in this study to calibrate root water uptake models.

Acknowledgements This research was funded by the Australian Research Council via the ARC Linkage Grant No. LP16160100649. The authors would like to extend their sincere appreciation for the

financial and technical support provided by both the City of Knox and FMG Engineering.

Funding Open Access funding enabled and organized by CAUL and its Member Institutions.

Data availability The datasets generated during and/or analysed during the current study are available from the corresponding author on reasonable request.

Open Access This article is licensed under a Creative Commons Attribution 4.0 International License, which permits use, sharing, adaptation, distribution and reproduction in any medium or format, as long as you give appropriate credit to the original author(s) and the source, provide a link to the Creative Commons licence, and indicate if changes were made. The images or other third party material in this article are included in the article's Creative Commons licence, unless indicated otherwise in a credit line to the material. If material is not included in the article's Creative Commons licence and your intended use is not permitted by statutory regulation or exceeds the permitted use, you will need to obtain permission directly from the copyright holder. To view a copy of this licence, visit <http://creativecommons.org/licenses/by/4.0/>.

References

- AS 1289 (2009) Methods for testing soils for engineering purposes, method 3.1.2, soil classification tests—determination of the liquid of a soil—one point Casagrande method (Subsidiary method). Standards Australia International Ltd, Sydney
- AS 1289 (2009) Methods for testing soils for engineering purposes, method 3.2.1, soil classification tests—determination of the plastic limits of a soil (Standard method). Standards Australia International Ltd, Sydney
- AS 2870 (2011) Residential slab and footings. Standards Australia International Ltd, Sydney
- Blight GE (2005) Desiccation of a clay by grass, bushes and trees. *Geotech Geol Eng* 23(6):697–720
- BOM (Bureau of Meteorology) (2021) Climate data online. <http://www.bom.gov.au/climate/data/>. Accessed 11 Oct 2021
- Burgess SSO, Adams MA, Turner NC, Beverly CR, Ong CK, Khan AAH, Bleby TM (2001) An improved heat pulse method to measure low and reverse rates of sap flow in woody plants. *Tree Physiol* 21:589–598
- Cameron DA (2001) The extent of soil desiccation near trees in a semi-arid environment. *Geotech Geol Eng* 19:357–370
- Cameron DA (2014) Expansive clays, collapsing sands, unbound pavement materials and unsaturated soil theory. In Proceedings of the 6th International conference on unsaturated soils. CRC Press, Sydney, Australia, pp 63–69
- Cameron DA, Beal NS (2011) Estimation of foundation movement and design of footing systems on reactive soils for the effects of trees. *J Aust Geomech* 46(3):97–113
- CPN International (2013) CPN 503 elite hydroprobe operating manual. InstroTek, Raleigh
- Dinka TM, Morgan CL, McInnes KJ, Kishné AS, Harmel RD (2013) Shrink–swell behavior of soil across a Vertisol catena. *J Hydrol* 476:352–359
- Fernández JE, Palomo MJ, Díaz-Espejo A, Clothier BE, Green SR, Girón IF, Moreno F (2001) Heat-pulse measurements of sap flow in olives for automating irrigation: tests, root flow and diagnostics of water stress. *Agric Water Manag* 51(2):99–123
- Fityus S, Cameron D, Driscoll C (2007) Observations of root architecture and their implications for modelling water movements in partially saturated soils. In: Yin Z, Yuan J, Chiu AF (eds) Proceedings of the 3rd Asian conference on unsaturated soils. Science Press, Nanjing, pp 207–213
- Fredlund DG, Xing A (1994) Equation for the soil–water characteristic curve. *Can Geotech J* 31(4):521–532
- Gadi VK, Hussain R, Bordoloi S, Hussain S, Singh SR, Garg A, Sekharan S, Karangat R, Lingaraj S (2019) Relating stomatal conductance and surface area with evapotranspiration induced suction in a heterogeneous grass cover. *J Hydrol* 568:867–876
- Garg A, Coo JL, Ng CWW (2015) Field study on influence of root characteristics on soil suction distribution in slopes vegetated with *Cynodon dactylon* and *Schefflera heptaphylla*. *Earth Surf Process Landf* 40:1631–1643
- Garg A, Leung AK, Ng CWW (2015) Comparisons of soil suction induced by evapotranspiration and transpiration of *S. heptaphylla*. *Can Geotech J* 52(12):2149–2155
- Gee GW, Campbell MD, Campbell GS, Campbell JH (1992) Rapid measurement of low soil water potentials using a water activity meter. *Soil Sci Soc Am J* 56(4):1068–1070
- Hignett C, Evett SR (2002) Neutron thermalisation. In: Dane JH, Clarke Topp G (eds) Methods of soil analysis, part 4, physical methods. Soil Sci Soc Am J, Madison
- Leong EC, Tripathy S, Rahardjo H (2003) Total suction measurement of unsaturated soils with a device using the chilled-mirror dew-point technique. *Geotechnique* 53(2):173–182
- Li J, Guo L (2017) Field investigation and numerical analysis of residential building damaged by expansive soil movement caused by tree root drying. *J Perform Constr Facil* 31(1):1–10
- Li J, Sun X (2015) Evaluation of changes of thornthwaite moisture index in Victoria. *J Aust Geomech* 50(3):39–49
- Li J, Cameron DA, Ren G (2014) Case study and back analysis of a residential building damaged by expansive soils. *Comput Geotech* 56:89–99
- Li J, Smith DW, Fityus SG, Shen D (2003) Numerical analysis of neutron moisture probe measurements. *Int J Geomech* 3(12):11–20
- Li J, Smith DW, Fityus SG (2003) The effect of a gap between the access tube and the soil during neutron probe measurements. *Aust J Soil Res* 41:151–164
- Li J, Zhou Y, Guo L, Tokhi H (2014) The establishment of a field site for reactive soil and tree monitoring in Melbourne. *J Aust Geomech* 49(2):63–72
- Li J, Zou J, Bayetto P, Barker N (2016) Shrink–swell index database for Melbourne. *J Aust Geomech* 51(3):61–76
- Loustau D, Berbigier P, Roumagnac P, Arruda-Pacheco C, David JS, Ferreira MI, Pereira JS, Tavares R (1996) Transpiration of a 64-year-old maritime pine stand in Portugal. 1. Seasonal course of water flux through maritime pine. *Oecologia* 107:33–42
- Nadezhkina N, Steppe K, De Pauw DJW, Bequet R, Cermak J, Ceulemans R (2009) Stem-mediated hydraulic redistribution in large roots on opposing sides of a Douglas-fir tree following localized irrigation”. *New Phytol* 184(4):932–943
- Ng CWW, Wang ZJ, Ni JJ (2020) Effects of plant morphology on root–soil hydraulic interactions of *Schefflera heptaphylla*. *Can Geotech J* 58(5):666–681
- Pandit R, Polyakov M, Tapsuwan S, Moran T (2013) The effect of street trees on property value in Perth, Western Australia. *Landsc Urban Plan* 110:134–142
- Plant L, Rambaldi A, Sipe N (2017) Evaluating revealed preferences for street tree cover targets: a business case for collaborative investment in leafier streetscapes in Brisbane, Australia. *Ecol Econ* 134:238–249
- Raven P, Evert RF, Eichhorn SE (1999) Biology of plants, 6th edn. W.H. Freeman Co., New York

34. Sun X, Li J (2023) A parametric study of the effect of trees on residential footing design on expansive soils. *Geotech Geol Eng.* <https://doi.org/10.1007/s10706-023-02400-0>
35. Sun X, Li J, Zhou AN (2017) Assessment of the impact of climate change on expansive soil movements and site classification. *J Aust Geomech* 52(3):39–50
36. Sun X, Li J, Cameron DA, Zhou AN (2021) Field monitoring and assessment of the impact of a large eucalypt on soil desiccation. *Acta Geotech* 17:1971–1984
37. Sun X, Li J, Cameron DA, Moore G (2022) Sap flow monitoring of two Australian native tree species in a suburban setting: implications for tree selection and management. *Plant Sci* 317:111194
38. Sun X, Li J, Cameron DA, Moore G (2022) On the use of sap flow measurements to assess the water requirements of three Australian native tree species. *Agronomy* 12(1):52
39. Zhou WH, He SY, Garg A, Yin ZY (2020) Field monitoring of suction in the vicinity of an urban tree: exploring termite infestation and the shading effects of tree canopy. *Acta Geotech* 15:1341–1361

Publisher's Note Springer Nature remains neutral with regard to jurisdictional claims in published maps and institutional affiliations.